

8. J. Bregman *et al.*, *Astron. Astrophys.* **187**, 616 (1987).
9. H. Campins and E. Ryan, *Astrophys. J.* **341**, 1059 (1989).
10. D. K. Lynch, R. W. Russell, J. A. Hackwell, M. S. Hanner, H. B. Hammel, *Icarus* **100**, 197 (1992).
11. M. S. Hanner, J. A. Hackwell, R. W. Russell, D. K. Lynch, *ibid.* **112**, 490 (1994).
12. M. S. Hanner, D. K. Lynch, R. W. Russell, *Astrophys. J.* **425**, 274 (1994).
13. The 11.2-μm feature also appeared less distinct on July 22 (R. W. Russell, D. Lynch, M. S. Hanner, M. Sitko, *IAU Circular* 6448).
14. We thank the staff of Palomar Observatory for assistance with the observations, G. Stacey and S. Stolovy for generously making a portion of their regularly scheduled observing time available for the nightly Hale-Bopp monitoring during June and August, and D. Yeomans for providing accurate comet ephemerides. The Spectro-Cam-10 detector was developed by the Space Infrared Telescope Facility program in conjunction with Cornell University and Rockwell International, and the development of the instrument was supported by NASA grant NAGW 2551 and the Department of Astronomy at Cornell University. M.S.H.'s research was conducted at the Jet Propulsion Laboratory, California Institute of Technology, under contract with NASA (Planetary Astronomy Program).

Telescope Facility program in conjunction with Cornell University and Rockwell International, and the development of the instrument was supported by NASA grant NAGW 2551 and the Department of Astronomy at Cornell University. M.S.H.'s research was conducted at the Jet Propulsion Laboratory, California Institute of Technology, under contract with NASA (Planetary Astronomy Program).

4 February 1997; accepted 27 February 1997

Optical Observations of Comet Hale-Bopp (C/1995 O1) at Large Heliocentric Distances Before Perihelion

Heike Rauer*, Claude Arpigny, Hermann Boehnhardt, François Colas, Jacques Crovisier, Laurent Jorda, Michael Küppers, Jean Manfroid, Kai Rembör, Nicolas Thomas

The activity of comet Hale-Bopp (C/1995 O1) was monitored monthly by optical imaging and long-slit spectroscopy of its dust and gas distribution over heliocentric distances of 4.6 to 2.9 astronomical units. The observed band intensities of the NH₂ radical and the H₂O⁺ ion cannot be explained by existing models of fluorescence excitation, warranting a reexamination of the corresponding production rates, at least at large heliocentric distances. Comparing the production rate of the CN radical to its proposed parent, HCN, shows no evidence for the need of a major additional source for CN in Hale-Bopp at large heliocentric distances. The dust and CN production rates are consistent with a significant amount of sublimation occurring from icy dust grains surrounding Hale-Bopp.

Most comets brighten sufficiently for detailed observations when their orbit brings them within 3 astronomical units (AU) from the sun. Our knowledge is, therefore, largely based on observations made when the activity is dominated by H₂O sublimation from the nucleus. Few comets have been observed far from the sun, where activity is driven by the second most abundant volatile, CO. Yet, studying the evolution of gas and dust activity over a large range of heliocentric distances, r_h , is important to characterize the composition and structure of the nucleus. The discovery of the bright comet Hale-Bopp (C/1995 O1) at about 7 AU has allowed us to observe the evolution of the comet over a large part of its orbit, as it approaches perihelion ($r_h = 0.91$ AU) on 1 April 1997.

We monitored Hale-Bopp from April to October 1996 with broadband filters and long-slit spectroscopy at optical wave-

lengths to determine its activity at r_h from 4.6 AU to 2.9 AU where the changeover from a CO-dominated to a H₂O-dominated activity takes place. We concentrated on

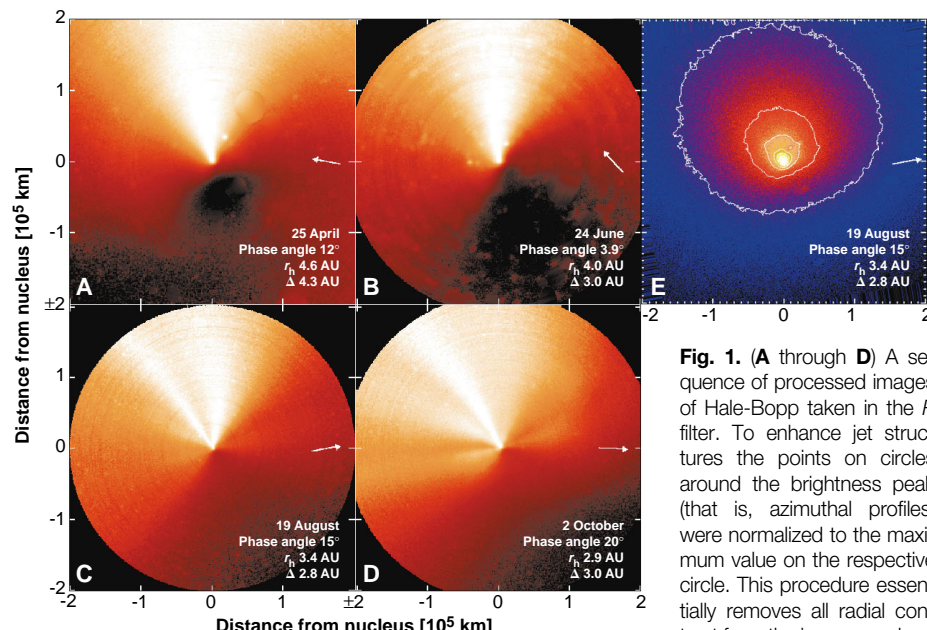


Fig. 1. (A through D) A sequence of processed images of Hale-Bopp taken in the *R* filter. To enhance jet structures the points on circles around the brightness peak (that is, azimuthal profiles) were normalized to the maximum value on the respective circle. This procedure essentially removes all radial contrast from the images and enhances azimuthal contrast. (E) Image of the CN emission at 3880 Å obtained on 20 August 1996. The exposure time is 10 min. An image taken with the blue continuum filter (ESO no. 510) was scaled and subtracted in order to remove the dust contribution. The images are rotated such that celestial North is upwards and East is to the left. The direction of the sun is indicated by an arrow.

H. Rauer and J. Crovisier, Observatoire de Paris-Meudon, 5, Place Jules Janssen, F-92190 Meudon, France. C. Arpigny and J. Manfroid, Institut d'Astrophysique, Avenue de Cointe 5, B-4000 Liège, Belgium.

H. Boehnhardt, Institut für Astronomie und Astrophysik, Ludwig-Maximilian-Universität München, Scheinerstrasse 1, D-81679 München, Germany.

F. Colas, Bureau des Longitudes, 77, Avenue Denfert Rochereau, F-75014 Paris, France.

L. Jorda, K. Rembör, N. Thomas, MPI für Aeronomie, Max-Planck-Strasse 2, D-37191 Katlenburg-Lindau, Germany.

*To whom correspondence should be addressed. E-mail: rauer@mesiob.obspm.fr

pects in some of the observed excitation bands.

The azimuthal distribution of the dust over 6 months (Fig. 2) showed that the prominent jet features in the coma (Fig. 1, A to D) represent enhancements in dust intensity of only 25% above the background level. The similarity between the overall distributions of dust over this 6-month period is striking. The maximum observed emission was directed roughly to the north, not toward the projected sun direction, as one would expect for isotropic emission from the sunward hemisphere of the nucleus. However, because of strong projection effects, it is difficult to quantify the angle between the direction of maximum emission and the solar vector. The north to south emission ratio of dust in the coma increased from 2.2 to 2.7 from June through October 1996. Images of the CN in the coma obtained in August 1996 showed a fan of CN emission that is also roughly toward the north (Figs. 1B and 2), with the maximum emission directed 20° to the west, in agreement with the overall dust distribution. Thus, the CN gas distribution confirms the asymmetric outgassing in Hale-Bopp. The north-to-south asymmetry could imply that the distribution of active areas on the surface is asymmetric, or there is a constantly illuminated pole in the

northern hemisphere. Alternatively, there could be a morning-afternoon asymmetry due to thermal lag of the nucleus, leading to increased sublimation from the afternoon side after the comet has warmed up as it rotates. This configuration would imply that the comet cannot be a slow rotator and its rotation axis would be close to the ecliptical plane, thus perpendicular to the orbital plane of the comet. A third possible explanation would be a projection effect of emission from several active areas emitting at the same position angle. The persistence of the emission pattern may be related to the small changes in the sun illumination and Earth viewing aspect angle of the active sources over the observed orbit arc. If the asymmetry is a projection effect, then we would expect to see significant changes in the azimuthal distribution before and through perihelion since the position of the sub-solar point on the nucleus changes rapidly during perihelion passage (5).

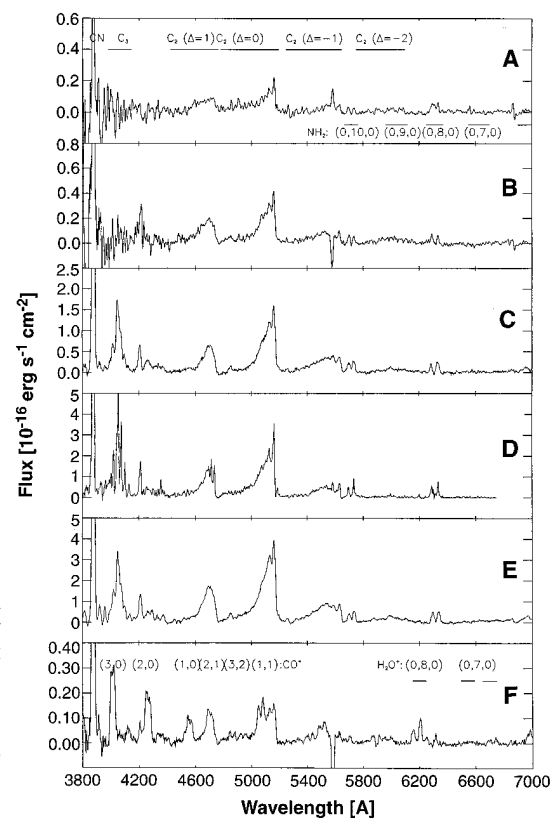
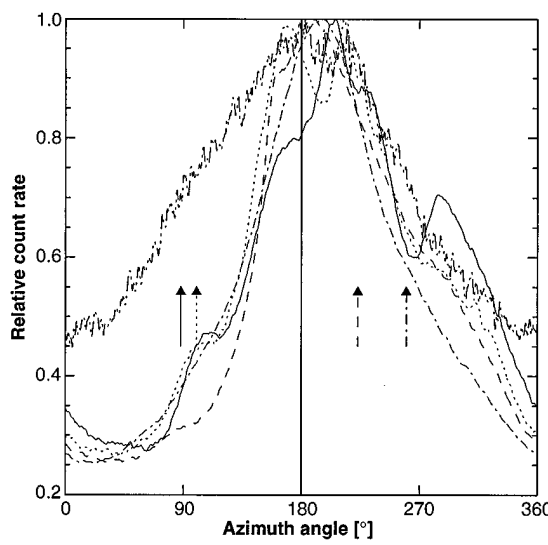
The continuum intensity can be related to the dust production rate, Q_{dust} , through the so-called A_{fp} parameter (6). We used the central part (400,000 km radius) of the R filter images (Fig. 1) to determine A_{fp} and compare it with the gas production rate as a function of time (Table 1). From the A_{fp} parameter Q_{dust} was computed (Table 1) using a standard model (7). The ratio $Q_{\text{dust}}/Q_{\text{gas}}$ decreased by

about a factor of 3 between April and October 1996. Such behavior is surprising, since one would expect Q_{dust} to increase with Q_{gas} . We estimated possible observational sources for this effect. Possible contamination of the R filter measurements by gaseous emissions tends to increase A_{fp} with decreasing r_h . The dust intensity from a comet is expected to be enhanced at small phase angles because of high backscattering efficiency. This might have increased the A_{fp} of Hale-Bopp in June by up to 50%, but no substantial effect is expected for phase angles larger than 10° (6). Therefore, the nearly constant temporal behavior of A_{fp} is real. A nearly constant behavior of A_{fp} at large r_h was also observed for comets Bowell 1980b and P/Halley (6, 8). From these and other comets observed at large r_h it was proposed (8) that a halo of icy grains could enhance the albedo of the observed particles and thus increase the measured A_{fp} . We suggest that a similar halo of icy grains existed in Hale-Bopp. The increase in Q_{dust} is then compensated by a decrease in albedo with decreasing r_h , as the icy grains sublime and refractory grains with lower reflectivity begin to dominate the dust emission. Indeed, icy grains were detected through their infrared signatures in Hale-Bopp at $r_h = 7$ AU (9). Fading grains had been proposed to explain relatively steep radial gradients ($\rho^{-1.5}$ in comet Tempel 2) of the dust intensity (10). To

Fig. 2 (left). An overlay of azimuthal profiles through R-filter images and a narrow-band CN filter image at a distance of 20,000 km from the brightness peak. The profiles are aligned in a frame of reference with celestial North at 180°, West at 90°. The direction of the sun is indicated by an arrow for the respective profiles. For the CN filter profile, the sun direction is the same as for the August R-filter profile.

Fig. 3 (right). Spectra of Hale-Bopp from 4.6 to 2.9 AU heliocentric distance. **(A)** 26 April 1996, 6:34 universal time (UT), $r_h = 4.6$ AU, $\Delta = 4.3$ AU; **(B)** 25 June 1996, 8:56 UT, $r_h = 4.0$ AU, $\Delta = 3.0$ AU; **(C)** 23 August 1996, 00:57 UT, $r_h = 3.3$ AU, $\Delta = 2.8$ AU; **(D)** 10 to 16 September 1996, $r_h = 3.1$ AU, $\Delta = 2.9$ AU; **(E)** 3 October 1996, 1:10 UT, $r_h = 2.9$ AU, $\Delta = 3.0$ AU. The spectra are averages of several columns in our two-dimensional (2D) long-slit spectra, taken slightly displaced from the nucleus [5 × 10⁴ to 6 × 10⁴ km, (B) at 1.3 × 10⁵ km] to increase the contrast between gas and continuum. The spectrum from September 1996 (D) is an average of several observations taken at the 1.93 m telescope at OHP, while all other spectra are from observations at the 1.52-m Danish telescope. Emission bands of CN, C₂, C₃, and NH₂ are present in all spectra taken. (The spectra from April and June had strong contamination by straylight in the blue spectral region which was subtracted. This led to an oversubtraction of faint C₃ emission.)

(F) is extracted from our 2D spectrum on 3 October 1996, at 10⁶ km in the anti-sunward direction and shows several emission bands of CO⁺ and H₂O⁺, in addition to CN and C₂ bands. Only the strongest CO⁺ emissions are indicated.



study if a similar gradient exists in Hale-Bopp, we have determined the radial dependence of the dust using the narrow-band continuum image from 20 August 1996. An intensity gradient of $\rho^{-1.10}$ is found between 3000 km and 50,000 km. This gradient is rather low for fading grains, and sublimating particles are therefore not strongly influencing the spatial dust distribution.

Hale-Bopp's optical spectrum changed as it approached the sun (11) (Fig. 3). At 3880 Å the strong emission bands of CN were seen in all our spectra. This band was the first gas emission detected in Hale-Bopp at 6.8 AU (12). However, for $r_h > 5$ AU, no other emissions at optical wavelengths were reported (13). It therefore came as a surprise that our spectra taken in April 1996, at $r_h = 4.6$ AU (Fig. 3A), showed emissions for C₂, C₃, and NH₂ that are usually seen in comets closer to the sun. For some of the molecules, such as C₃ and NH₂, this is the largest r_h they have yet been observed.

As Hale-Bopp moved closer to the sun ($r_h = 3.3$ AU, Fig. 3C), the first emissions of the ions of the major cometary constituents, H₂O⁺ and CO⁺ appeared [CO⁺ was first reported on 17 August 1996 (14)]. Their sublimating parents, CO and H₂O (inferred from OH), were detected at $r_h > 6$ AU and $r_h = 4.8$ AU, respectively (15, 16). It is likely that the strong dust continuum and some time-variability in the ion tail are responsible for the relatively late detection of the ion emissions. At 3.1 AU, the weak emissions from CH and CH⁺ appeared at 4310 Å and 4235 Å, respectively.

To derive gas production rates from the observed line fluxes, a molecular excitation model is needed in combination with a coma outflow model. Both models make

several assumptions, that may not be valid for Hale-Bopp at large r_h . Determination of relative band ratios of emission features is useful for testing the validity of fluorescence excitation models, which are used to translate the observed fluxes into column densities. The mean ratio of the C₂ ($\Delta v = 1/\Delta v = 0$) bands is found to be 0.53 ± 0.05 , in agreement with the theoretical ratio of 0.54 (17). The emission bands of NH₂ in the spectra of Hale-Bopp showed an anomaly at large r_h . Bands with an even upper vibrational quantum number v'_2 , (0, 10, 0) and (0, 8, 0), are much stronger than bands with an odd v'_2 . The odd bands, (0, 9, 0) and (0, 7, 0), do appear near $r_h \approx 3.1$ AU and increase somewhat in strength thereafter, but they remain faint until 2.9 AU. For instance, the (0, 9, 0) band is at least six times weaker than expected from fluorescence excitation models whereas the observed (0, 10, 0)/(0, 8, 0) intensity ratio is about 1.2, close to the predicted value (18) {contamination of the (0, 8, 0) band by [OI] emission is negligible}. For this ratio we find no obvious trend with r_h between 4.6 and 2.9 AU. Production rates of NH₂ are used to derive the NH₃ abundance in comets. Because the ratio of NH₃ to N₂ and CO is temperature-dependent, and can therefore help define the formation conditions of comets and the amount of chemical processing, reliable Q_{NH_2} values are needed. The anomalous NH₂ emissions seen in Hale-Bopp beyond about 3 AU suggest that it will be necessary to reexamine the validity of fluorescence excitation models and therefore the production rates derived from these models. Spectra from Hale-Bopp near perihelion are required to verify if the excitation conditions are then similar to those

seen in other comets and are in agreement with models applied near $r_h = 1$ AU.

A similar anomaly in excitation was observed for H₂O⁺. At 3.3 AU only the (0, 8, 0) band is present, although the (0, 7, 0) band near 6550 Å should be equally strong (19). The (0, 7, 0) band appeared weakly at 2.9 AU. Because NH₂ and H₂O⁺ have the same spectroscopic structure it is not surprising that their emission bands behaved in the same manner, but their excitation at large r_h cannot be explained by current excitation models (18, 19).

Because of the selection rules for NH₂ and H₂O⁺ transitions, the even v'_2 bands only involve even lower rotational levels, and the odd v'_2 bands only odd lower levels (20). This might explain why the ratio of bands with even v'_2 is close to the predicted value, while the ratio of odd to even v'_2 is not. However, there is apparently no reason why even and odd lower states in NH₂ should not be more or less equally populated at large r_h . The different molecular structure of their parents, NH₃ and H₂O, and the different formation processes, photodissociation and photoionization, make a different level population caused by the creation process unlikely. An additional excitation mechanism, like collisions, might play a role only in the innermost regions of the coma. Instead, we think that the solution will be found through a detailed study of the radiative processes as they apply to the particular molecular structure of NH₂ and H₂O⁺. This suggestion is based on evidence indicating that these molecules are rotationally extremely cold in Hale-Bopp at large r_h .

To derive production rates we used the Haser model (21) which assumes isotropic outgassing at constant speed and photodissociation of the parent and daughter molecules. Although this model is not strictly valid, it serves as a good reference model when comparing different observations. We used a gas

Table 1. The Af_p parameter, dust production rate, Q_{dust} , and the ratio of dust production to total gas production rate, Q_{gas} [determined by adding the CO and OH production rates from radio observations (25)]. ϕ denotes the phase angle.

Date	r_h [AU]	ϕ [°]	Af _p [m]	Q_{dust} [10^3 kg s^{-1}]	$Q_{\text{dust}}/Q_{\text{gas}}$
26.4.1996	4.6	12	450 ± 70	18.7	6.0
25.6.1996	4.0	4	600 ± 90	27.4	3.8
20.8.1996	3.4	15	490 ± 70	33.3	3.0
3.10.1996	2.4	19	630 ± 90	58.8	2.3

Table 2. Gas production rates, Q . r_h and Δ denote the heliocentric and geocentric distance, respectively.

Date	r_h [AU]	Δ [AU]	$Q(\text{CN})$ [10^{27} s^{-1}]	$Q(\text{C}_2)$ [10^{27} s^{-1}]	$Q(\text{C}_3)$ [10^{27} s^{-1}]	$Q(\text{NH}_2)$ [10^{27} s^{-1}]
26.4.1996	4.6	4.3	0.2 ± 0.1	0.6 ± 0.3	—	0.2 ± 0.1
25.6.1996	4.0	3.0	0.6 ± 0.2	0.7 ± 0.2	—	0.4 ± 0.2
23.8.1996	3.3	2.8	0.9 ± 0.2	1.4 ± 0.2	—	0.6 ± 0.2
10–16.9.1996	3.1	2.9	1.9 ± 0.7	1.9 ± 0.7	0.12 ± 0.021	1.1 ± 0.4
3.10.1996	2.9	3.0	1.3 ± 0.4	2.2 ± 0.4	0.24 ± 0.04	1.0 ± 0.4

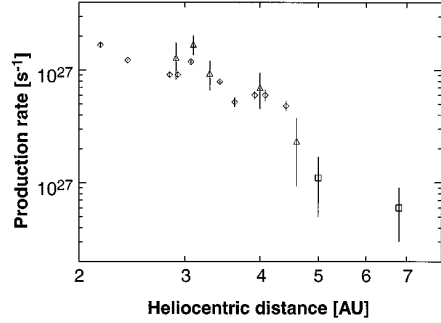


Fig. 4. CN production rate over heliocentric distance. Rates at 6.8 AU and 5.0 AU (squares) are taken from (4, 5), all other rates are from this study (triangles). The CN production rate shows a strong increase around 4.6 AU. For comparison, the production rates of HCN (18), the probable parent of CN, are shown (diamonds).

velocity of 1 km s^{-1} at 1 AU and scaled it to the observed distance by $r_h^{-0.5}$. The destruction scale lengths for the parent and daughter molecules were determined from observations near the sun and it is unclear if they are applicable at large r_h . We tested if three different sets of scale lengths (8, 22, 23) could approximate our spatial emission profiles from long-slit spectra in Hale-Bopp. The scale lengths given by (22) approximate the observed profiles the best, although values by (23) give similar results (24). Straylight prevented us from deriving Q_{C_3} at large r_h . However, Q_{C_3} was derived from the spectrum taken at OHP, which is free from such straylight (Table 2). The rates for NH_2 were derived from the (0, 10, 0) band, although the unusual excitation of NH_2 means that rates may not be valid. For August, a lower limit for the CN production rate was calculated from our CN frame. This rate is 30% below the value derived from the spectra, which represents good agreement giving the various uncertainties in parameters. From the production rates (Table 2) derived under the simplifying assumptions made above, we can see the general trend of activity and determine the mean ratio of C_2 to CN. With a mean $\log(C_2/\text{CN}) = 0.1 \pm 0.2$ between 4 to 3 AU, Hale-Bopp falls into the range of typical comets as defined by (8).

Observations of CN gave us the largest coverage of gas activity in Hale-Bopp from 7 to 3 AU (Fig. 4). While the gas production at $r_h \geq 5$ AU was low (12, 13), it increased between 5 and 4.6 AU. At $r_h = 4.6$ AU, we also detected C_2 , C_3 , and NH_2 . The increase in CN production rate coincides with the first detection of OH at 4.8 AU (16), and its subsequent strong increase (25). It is therefore suggestive to relate the enhanced Q_{CN} , which is indicative for that of its main parent HCN, to the increase in H_2O sublimation.

The increase in Q_{HCN} with increasing $Q_{\text{H}_2\text{O}}$ could be explained by additional HCN provided from the nucleus surface or by an additional sublimation source, such as icy-dust grains in the coma. The Infrared Satellite Observatory measured a color temperature of $T = 160 \text{ K}$ in the range of 6 to 12 μm at $r_h = 4.6$ AU (26), at the same time as Q_{CN} increased. The free sublimation temperature of H_2O ice is 152 K (27), suggesting that the increase in Q_{CN} was linked to the sublimation of H_2O ice and not to the sublimation of pure HCN ice (which sublimes at 95 K). An increase in Q_{CO} was observed near $r_h = 4.5$ AU (25, 28), but by a much smaller amount than Q_{CN} . This is not surprising in view of the large amount of CO coming directly from the nucleus. Evidence for H_2O sublimation from grains has also been found in radio observations of OH (25).

From a recent comparison of many comets, and previous observations, it was proposed that sublimation of relatively pure H_2O ice

grains could explain the observed small $Q_{\text{CN}}/Q_{\text{OH}}$ ratio seen in comets with perihelia ≥ 2.5 AU (8). However, such pure H_2O ice grains cannot explain the observed increase in Q_{CN} around 5 AU in Hale-Bopp. We propose that icy grains in Hale-Bopp, beginning to sublime around 5 AU, are relatively fresh and have a composition similar to the nucleus surface. Such grains would serve as a natural source for the additional CN observed at 5 AU.

Observations of CN jets in Halley and comparison to Q_{HCN} led to the proposition that CN might be partially released from small dust grains (29). Comparing the gas and dust distribution (Fig. 2), CN does not appear to be related to the spatial distribution of dust to first order. The distribution of CN is, however, consistent with the HCN distribution inferred from sub-mm observations (25). This suggests that visible dust is not a significant source of CN in Hale-Bopp. (Evaluation of the C_2 distribution shows qualitatively the same spatial distribution as CN, implying a similar distribution of its source.) However, the possibility of CN coming from small grains, invisible at optical wavelength, or from additional parent molecules, remains (8). Two additional parent molecules for CN, CH_3CN and HNC, have recently been discovered in comet Hyakutake (C/1996 B2) (30). Measurements in Hale-Bopp give a ratio of CH_3CN to HCN of $12 \pm 2\%$ at 3 AU, and about 20% HNC to HCN at 1.5 AU (25). Thus, about 30% of CN can come from these additional volatiles retained in the ice. To study if an additional source is required for Hale-Bopp, we compare Q_{CN} and Q_{HCN} (Fig. 4). From these measurements, we conclude that a major additional source of CN (for example, from the refractory component) is not required in Hale-Bopp in the r_h range studied.

REFERENCES AND NOTES:

1. We used the Danish Faint Object Spectrograph (DFOSC), a focal reducer-type instrument which allowed us to switch between spectra (3700 to 7000 Å; resolution: April and June: 15 Å, August and October: 18 Å), and imaging. The field-of-view was ≈ 13 arc min. The slit was aligned with the sun-comet axis.
2. Because no special filters centered on the cometary emissions were available to us, we chose filters from the standard ESO filters set [no. 514 at 3849 Å (band width 87 Å) for CN; no. 430 at 5117 Å (band width 56 Å) for C_2 ; filter no. 510 at 4467 Å (band width 56 Å) has been used for continuum subtraction].
3. We used the medium-resolution spectrograph CARELC in the range 3600 to 6800 Å (resolution: 7 Å). The slit length was 5 arc min. Spectra were taken with different slit orientations and averages obtained from these spectra.
4. Z. Sekanina and H. Boehnhardt, *IAU Circular* 6542 (1997); M. R. Kidger *et al.*, in preparation.
5. Dramatic changes in dust distribution were observed recently [for example, see J. Lecacheux and F. Collas, *IAU Circular* 6560 (1997)].
6. M. F. A'Hearn *et al.*, *Astron. J.* **89**, 579 (1984). Here, A is the albedo, f is the filling factor (ratio between total cross section of grains and area of the field of view), and ρ is the radius of the circular field of view.
7. The calculations are based on isotropic hydrodynamical modeling of the gas-dust interaction using CO and H_2O molecules weighted by their respective mass production rates. This model accounts for the variation of thermal gas velocity with nucleus temperature as $280 \text{ K}/\sqrt{r_h}$. To correct for the dependence of magnitude on phase angle, a factor of 0.03 mag/degree was used, as measured in comet Bowell at 3.7 to 5.6 AU. [R. L. Newburn and H. Spinrad, *Astron. J.* **90**, 2591, (1985); J. F. Crifo, *Astron. Astrophys.* **187**, 438, (1987); K. Meech and D. Jewitt, *ibid.*, p. 585.]
8. M. F. A'Hearn, R. L. Millis, D. G. Schleicher, D. J. Osip, P. V. Birch, *Icarus* **118**, 223 (1995).
9. J. K. Davies *et al.*, *ibid.*, in press.
10. D. Jewitt, in *Comets in the Post-Halley Era*, R. L. Newburn, M. Neugebauer, J. Rahe, Eds. (Kluwer, Dordrecht, 1991) pp. 19–65.
11. All spectra were bias-subtracted, flatfielded, and extinction-corrected. The contribution from the night sky was determined from separate sky exposures. Variability in intensity of the [OI] emission at 5577 Å led to under- and oversubtraction in some cases. The underlying continuum of solar light reflected by the cometary dust was subtracted using a solar atlas [R. L. Kurucz *et al.*, *Sunspot*, National Solar Observatory, (1984)] smoothed to the resolution of the cometary spectra, or using spectra of jovian satellites, when possible. Absolute calibration was performed using standard stars observed on the same night.
12. A. Fitzsimmons and I. M. Cartwright, *Mon. Not. R. Astron. Soc.* **278**, L37 (1996).
13. ———, *IAU Circular* 6361 (1996).
14. K. Jockers, T. Credner, N. Karpov, A. Sergeev, *IAU Circular* 6468 (1996).
15. N. Biver *et al.*, *Nature* **380**, 137 (1996); D. Jewitt, M. Senay, H. Matthews, *Science* **271**, 1110 (1996).
16. H. A. Weaver *et al.*, *IAU Circular* 6376 (1996).
17. M. F. A'Hearn *et al.*, *Icarus* **64**, 1, (1985).
18. A. Tegler and S. Wyckoff, *Astrophys. J.* **343**, 445 (1989) and references therein.
19. B. L. Lutz, *Astrophys. J.* **315**, L147 (1987).
20. C. Arpigny, in *Molecules and Grains in Space*, AIP Conf. Proc. **312**, I. Nenner, Ed. (AIP Press, New York, 1994), pp. 205–239.
21. L. Haser, *Bull. Acad. R. Belg., Classes Ser.* **5**, 43 (1957).
22. A. Cochran, E. S. Barker, T. F. Ramseyer, A. D. Storrs, *Icarus* **98**, 151 (1992).
23. U. Fink and M. Hicks, *Astrophys. J.* **459**, 729 (1996).
24. In particular for C_2 , for which the scale lengths and its scaling with r_h differ significantly in the literature, this is an illustration of how difficult it is to constrain a unique set of parameters. Moreover, although the predicted profiles are similar, the resulting production rates can differ by 30% depending on the scale lengths used. We chose for all species the scale lengths given by (22); g -factors for C_3 from (8), for CN from: D. Schleicher, thesis, University of Maryland (1983); others from (22).
25. N. Biver *et al.*, *Science* **275**, 1915 (1997).
26. J. Crovisier *et al.*, *Astron. Astrophys.* **315**, L385 (1996).
27. T. Yamamoto, *ibid.* **142**, 31, (1985).
28. M. Womack, D. Suswal, S. A. Stern, D. Slater, M. Festou, *Bull. Am. Astron. Soc.* **28**, 1091 (1996).
29. M. F. A'Hearn *et al.*, *Nature* **324**, 649 (1986).
30. A. Dutrey *et al.*, *IAU Circular* 6364 (1996); W. M. Irvine *et al.*, *Nature* **383**, 418 (1996).
31. This paper is based on observations at the European Southern Observatory (ESO), Chile (prop. 57.F-0396), and the Observatoire de Haute Provence, France. We gratefully acknowledge the collaboration with members of the ESO ROSETTA/ISO target comets imaging team in the context of their observing programs at ESO [57.F-0274, 58.F-0431 (ESO time)], whose members are H. Boehnhardt, L. Colangeli, G. Cremonese, J. Crovisier, M. Fulle, L. Jordá, H. Rauer, H. Rickman, R. Schulz, G. Schwehm, and R. M. West. We thank also V. Buat and D. Burgarella, who gave us some of their observing time. H.R. acknowledges the support of an European Space Agency external research fellowship.

6 February 1997; accepted 27 February 1997